Available online at www.sciencedirect.com
ScienceDirect
Cement and Concrete Research 38 (2008) 325–336
Cement and Concrete Research

Thermodynamics of crystallization stresses in DEF

Robert J. Flatt [a,*], George W. Scherer [b]

[a] Sika Technology AG, CH-8048 Zürich, Switzerland
[b] Department of Civil & Env. Eng., Princeton University, Princeton NJ 80540, USA

Received 15 December 2006; accepted 18 October 2007

Abstract

The thermo-mechanics of damage during delayed ettringite formation have been examined. A thermodynamic approach is used to evaluate the supersaturation under which ettringite may form and the crystallization pressures that may result. From these stresses at the pore scale and with the amount of ettringite forming, an average hydrostatic tensile stress in the solid is calculated and compared to the tensile strength of tested samples.

Results indicate that, when the loading rate dependence of tensile strength is taken into account, it is possible to rationalize factors that do or do not contribute to damage, such as ettringite content, temperature and fly-ash content. Although a number of important assumptions are made and clearly indicated in the paper, the results do open a new perspective onto durability studies which goes beyond the sole case of delayed ettringite formation.

1. Introduction

Delayed ettringite formation (DEF) can be a process that is responsible for loss of durability of cementitious materials. There has been extensive debate in the literature about the actual mechanism that leads to such damage, as summarized by Taylor et al. [1]. Despite diverging views on the subject, it is generally accepted that the cementitious material must be cured at temperatures above around 70 °C. After such curing, many samples are observed to expand at ambient temperature under high humidity, a process associated with microcracking of the cement paste.

It is not the object of this work to discuss all the parameters that may influence the magnitude of this expansion, but rather to examine the thermodynamics of the crystallization of ettringite (calcium alumino trisulfate of composition $Ca_6Al_2(SO_4)_3(OH)_{12}(H_2O)_{26}$) which is often pointed to as the basic mechanism responsible for this expansion [2,3]. The treatment focuses on estimating the dependence of crystallization stresses on the storage temperature following heat curing. It also deals with the influence of solution composition on the magnitude of these stresses. The results suggest that addition of appropriate additives during sample preparation might limit the degree of expansion.

Before presenting our estimations of stresses generated during DEF, we must recall some aspects of thermodynamics of crystallization pressure, their link to stresses and possible failure. A more detailed discussion of these has already been given by Scherer [2].

For crystallization to cause damage, the crystal must be in a highly supersaturated solution. If the crystal is in a pore that is not completely filled, then it will grow to consume the supersaturation. Damage can occur from crystallization in a large pore, if this pore gets completely filled and the liquid film between the crystal and the pore wall remains highly supersaturated [4,5,2,3]. Alternatively damage can occur by crystals growing in mesopores without these having to be filled, and this is what is expected to take place in the case of DEF [1]. Over time, however, the system thermodynamically favors formation of crystals in larger pores which reduces crystallization pressure. Transport limitations do not allow the system to reach this situation immediately, which is why DEF can be damaging without ettringite having to fill all large pores in the samples. In this paper, we do not deal with transient stresses, but only with the initial (peak) stresses that occur before redistribution of crystals into larger pores.

* Corresponding author.
E-mail address: flatt.robert@ch.sika.com (R.J. Flatt).

0008-8846/$ - see front matter © 2007 Elsevier Ltd. All rights reserved.
doi:10.1016/j.cemconres.2007.10.002

The reason ettringite crystallization is blamed for expansion of heat-cured samples is that, at elevated temperatures, this phase becomes increasingly unstable with respect to monosulfate, a calcium alumino monosulfate of composition $Ca_4Al_2(SO_4)(OH)_{12}(H_2O)_6$, and a solution of increased calcium sulfate concentration [6,7]. In the case of cement paste, there is increasing evidence that not all the calcium sulfate resulting from ettringite increasing solubility remains in the pore solution, but that a significant part is adsorbed onto the surface of the C–S–H phase [1]. Indeed, after heat curing, no ettringite is observed by XRD, but it reappears after exposure at ambient temperature in moist conditions. It is expected that under those conditions, crystallization of ettringite occurs in a highly supersaturated solution and induces large stresses when growth occurs in small pores [1].

Sodium sulfate, though a simpler mineral, also causes large damage when a sample, after heat treatment, is stored at ambient temperature in humid conditions. In this case, it has been shown that the mechanism involves the coupled dissolution of metastable phase B (thenardite) formed during heating, followed or accompanied by precipitation of the phase A (mirabilite) that is stable at the storage conditions [27]. If the dissolution of B stops because its solubility limit is reached before the nucleation of A, then the solution composition from which A crystallizes can be approximated by the equilibrium concentration of phase B, allowing supersaturation and crystallization stresses to be estimated.

In what follows, we use a similar approach to estimate the supersaturation in DEF with respect to ettringite. For this we need to identify the phases that can be considered to be in equilibrium with the solution and which allow us to express supersaturation in terms of equilibrium constants of those phases, rather than ion activities. This approximation is useful since the ionic concentration at the location of ettringite formation is not accessible. Thus, the approach presented in this paper provides some rationale for the estimation of this value, which in turn dictates the magnitude of the stresses resulting from crystal growth in confined media.

2. Background

2.1. Crystallization pressure

Various estimations of crystallization pressure can be found in the literature, the first of which dates back to Correns [8][1]. The magnitude of crystallization pressure depends on the shape of the pore and supersaturation. It can also be written in terms of pore size when supersaturation is expressed as the size of the smallest crystal that can exist in the defined solution [4].

The growth of a large crystal in a supersaturated solution can be prevented by applying directly on the crystal a pressure given by: [8], Buil (1985), Scherer (2002), [2,3,10]:

$$\sigma_C = \frac{R_g T}{v_{crystal}} \ln\left(\frac{Q}{K}\right) \quad (1)$$

where R_g is the gas constant, T is the absolute temperature, $v_{crystal}$ is the molar volume of the crystal (660.6 cm^3/mol for ettringite), Q/K is the supersaturation, Q is the ion activity product and K is the equilibrium constant.

Eq. (1) represents the hydrostatic stress that the matrix has to apply to suppress growth of the crystal. The resulting distribution of stresses in the solid, and the likelihood of those stresses to nucleate or propagate cracks, is difficult to predict. Coussy has shown how one can approach such situations in the case of freezing [11] and drying [12]. Applying such models requires materials parameters that we don't know, and involves assumptions regarding the criterion for failure. For the present, we will adopt a simplified model for calculating the tension in the porous matrix which we believe is sufficient to provide useful estimates. We recognize, of course, that for a given well-characterized sample, better predictions could be made by more elaborate calculations.

For an isolated crystal, the tensile hoop stress at the surface of the pore is given by:

$$\sigma_\theta = \sigma_C f(\phi_C) \quad (2)$$

where ϕ_C is the volume fraction of crystals exerting pressure in the sample and $f(\phi_C)$ for a crystal in a cylindrical pore is given by [4]:

$$f(\phi_C) = \frac{1+\phi_C}{1-\phi_C} \quad (3)$$

and for a crystal filling a spherical pore with small entries, it is given by [13]:

$$f(\phi_C) = \frac{1+2\phi_C}{2(1-\phi_C)} \quad (4)$$

However, the stress that is more relevant for establishing a damage criterion is the average hydrostatic tensile stress σ in the solid. The corresponding expressions can be derived from the stresses in a pressurized vessel [14] and are found to be:

$$\sigma = \sigma_C\, g(\phi_C) \quad (5)$$

where $g(\phi_C)$ is given by the following expression for the cylindrical pore

$$g(\phi_C) = \frac{2}{3}\left(\frac{\phi_C}{1-\phi_C}\right) \quad (6)$$

and for the filled large spherical pore with small entries it would be:

$$g(\phi_C) = \left(\frac{\phi_C}{1-\phi_C}\right) \quad (7)$$

From Eq. (5) we see that the crystallization pressure that can damage a material of given strength varies as $1/g(\phi_C)$. As shown in Fig. 1, this factor depends strongly on the volume fraction of crystals exerting pressure. Higher values in that figure mean more crystallization pressure is needed to compensate for the smaller volume fraction of crystals exerting pressure. Furthermore, crystals forming in cylindrical pores

[1] See also a commented translation of the original work that led to that paper [9].

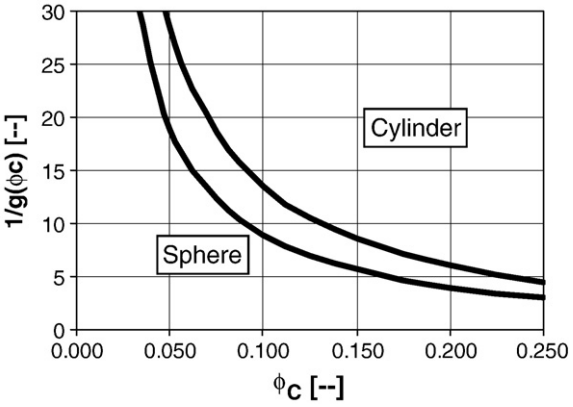

Fig. 1. Damage criterion given in terms of the ratio between the equilibrium crystallization pressure and tensile strength as a function of the volume fraction of crystals. The lower curve corresponds to filled spherical pores with small entries and the upper curve corresponds to cylindrical pores.

require higher crystallization pressures than those in larger pores with small entries.

For this stress to damage a material it must be able to propagate existing flaws. This issue was discussed for the two dimensional case by Scherer [4], based on a theory developed by Lu et al. [15]. In the case where a small number of crystals have nucleated, the hoop stress induced by crystallization pressure that is required to propagate an adjacent flaw of size c is given by:

$$\overline{\sigma}_\theta = \sqrt{\frac{8}{\pi}}\left(1+\frac{c}{R}\right)^{3/2}\frac{K_{lc}}{\sqrt{c}} \tag{8}$$

where R is the radius of the region over which the stress acts and K_{lc} is the critical stress intensity factor. Here, $\overline{\sigma}_\theta$ is the hoop stress integrated over the volume with an appropriate weighting factor [15].

In the case of DEF, however, we expect that nucleation and growth will occur abundantly and throughout the sample volume. As a result, the tensile stress is uniformly applied throughout the sample, and the fracture criterion can be written in terms of tensile strength σ_T [16]:

$$\sigma = \sigma_T = \frac{K_{lc}}{2\sqrt{c/\pi}} \tag{9}$$

This indicates that the stress required for propagating flaws decreases as flaw size increases. In what follows we undertake various estimations of supersaturation to evaluate whether or not destructive stresses can be reached.

2.2. Mechanical resistance to crystallization pressure

2.2.1. Conversion of flexural to tensile strength

The above equations link crystallization damage and tensile strength. Two convenient ways of determining tensile strength of cementitious materials are indirect tests. The first, a splitting test, uses a well established expression between the load needed to split a horizontal cylinder and tensile strength. The second is bending strength. It uses somewhat less well defined relations. In this case, a model code CEB/FIP can be used, which proposes the following relation between bending and tensile strength [26]:

$$R_t = R_f \frac{a\left(\frac{h}{100}\right)^{0.7}}{1+a\left(\frac{h}{100}\right)^{0.7}} \tag{10}$$

where R_t is the strength from a direct tensile test, Rf is the strength form a flexural test, h is the sample height in mm and a is a fragility factor.

The value of a is taken to be 1.5 for standard concrete and 2 when the matrix is brittle. In this paper we will be illustrating our arguments with mortar bars. The brittle matrix is the case we assume in absence of any more specific information.

2.2.2. Time dependent strength

In the process of DEF, damage appears after a rather substantial period of time. This is typically on the order of 2–3 months for mortars discussed later in this paper. From EDX examinations, it is known that ettringite can appear well before expansion is detected [19]. Thus the relevant strength for these tests corresponds to very slow loading rates. It is known that loading rates have an effect on concrete strength and, while the issue is rather delicate in that the question of creep should also be considered, there are estimates that for tensile strengths, a low loading rate limit can lie substantially below values obtained at standard loading rates in the laboratory. Rheinhardt and Cornelissen [17] find, for example, that the tensile strength drops to about 60% of its nominal (standard measured) value in tests that last 24 h. They propose the following relation to estimate the time dependence of such changes on their samples:

$$Log_{10}(t_f) = 13.63 - 14.46\frac{\sigma_f}{f_{ctm}} \tag{11}$$

where t_f is the time to fracture, σ_f is the load at fracture and f_{ctm} is the tensile strength determined under normal laboratory conditions.

2.3. Estimation of supersaturation

The solubility product of ettringite may be written as:

$$Q_{ettringite} = a^6_{Ca^{2+}} a^2_{Al(OH)_4^-} a^3_{SO_4^{2-}} a^4_{OH^-} a^{26}_{H_2O} \tag{12}$$

Let us assume that the solution is saturated with respect to monosulfate (metastable) at room temperature. The equilibrium condition for monosulfate dissociation can be written as:

$$K_{monosulfate} = a^4_{Ca^{2+}} a^2_{Al(OH)_4^-} a_{SO_4^{2-}} a^4_{OH^-} a^6_{H_2O} \tag{13}$$

Monosulfate is actually liable to have some of its sulfate ions substituted by either hydroxyls or carbonates. This situation leads to more complex expressions that will be dealt with later. In the absence of any substitution, the supersaturation with respect to ettringite can be written as:

$$\frac{Q_{ettringite}}{K_{ettringite}} = \frac{K_{monosulfate}}{K_{ettringite}} a^2_{Ca^{2+}} a^2_{SO_4^{2-}} a^{20}_{H_2O} \tag{14}$$

This equation indicates that the assumption that monosulfate is in equilibrium is not sufficient to define the supersaturation with

respect to ettringite. The activities of calcium, sulfate and water still remain to be determined. This differs from the case of sodium sulfate mentioned before in which all the ion activities are included in the solubility product of the metastable phase.

For the case we are concerned with, the remaining activities could be calculated from analysis of the pore fluid or possibly from the equilibrium requirements of other phases present in the system. In the first case, a pore solution would have to be extracted at a given point in time and one analysis per sample type and point in time would be needed. Of course, the liquid extracted must be representative of the solution concentration at the location where ettringite responsible for expansion is growing. In the second case, one must decide which relevant phases may be considered to be in equilibrium and in the vicinity of the monosulfate. The advantage of this approach is that it provides a result that is not sample specific. In the absence of measurements of the composition of the pore solution, it is a useful first step to estimate ranges of crystallization pressures.

What we need is to identify a phase that will give both calcium and sulfate activities at the same time. Furthermore both ions must have the same ratio in that solubility product.

2.4. Gypsum equilibrium

At first sight, gypsum would be a good candidate for the above requirements. However, by the end of the heat treatment, there is barely any gypsum left in the system. If gypsum were left it would probably mean that the decomposition to monosulfate may not occur extensively and the damage from DEF would not be extensive. Despite this, we use the condition of gypsum equilibrium to estimate an upper bound of crystallization pressure.

The equilibrium requirement for gypsum may be written as:

$$K_{\text{gypsum}} = a_{Ca^{2+}} a_{SO_4^{2-}} a_{H_2O}^2 \tag{15}$$

Substitution into Eq. (14), gives:

$$\frac{Q_{\text{ettringite}}}{K_{\text{ettringite}}} = \frac{K_{\text{monosulfate}}\ K_{\text{gypsum}}^2}{K_{\text{ettringite}}} a_{H_2O}^{16} \tag{16}$$

2.5. Hydrogarnet equilibrium

Taylor (2001) reports that heat treated samples often contain hydrogarnet, $Ca_3Al_2(OH)_{12}$. Though this phase does not contain sulfates, we will see how it can be used to evaluate the activity product of calcium and sulfate in solution.

The equilibrium requirement for hydrogarnet may be written as:

$$K_{\text{hydrogarnet}} = a_{Ca^{2+}}^3 a_{Al(OH)_4^-}^2 a_{OH^-}^4 \tag{17}$$

If we now take the ratio of the expression for the monosulfate equilibrium, Eq. (13), to that of hydrogarnet, Eq. (17), we obtain:

$$\frac{K_{\text{monosulfate}}}{K_{\text{hydrogarnet}}} = a_{Ca^{2+}} a_{SO_4^{2-}} a_{H_2O}^6 \tag{18}$$

This provides us with the activity product between calcium and sulfate. If Eq. (18) is substituted into the Eq. (14), the supersaturation of ettringite turns out to depend only on water activity and on equilibrium constants (themselves functions of temperature);

$$\frac{Q_{\text{ettringite}}}{K_{\text{ettringite}}} = \frac{K_{\text{monosulfate}}^3}{K_{\text{ettringite}}\ K_{\text{hydrogarnet}}^2} a_{H_2O}^8 \tag{19}$$

2.6. Portlandite equilibrium

One phase that can be safely considered to be at equilibrium is portlandite. Despite the fact that using this phase does not eliminate sulfate activity and introduces hydroxide activity, it provides useful information concerning the effect of hydroxide activity. Portlandite equilibrium may be written as:

$$Q_{\text{portlandite}} = a_{Ca^{2+}} a_{OH^-}^2 \tag{20}$$

Substitution in Eq. (14) gives:

$$\frac{Q_{\text{ettringite}}}{K_{\text{ettringite}}} = \frac{K_{\text{monosulfate}}\ K_{\text{portlandite}}^2}{K_{\text{ettringite}}} \frac{a_{SO_4^{2-}}^2}{a_{OH^-}^4} a_{H_2O}^{20} \tag{21}$$

Unlike Eqs. (16) and (19), this expression requires calculation of ion activities in the pore solution.

2.7. Thermodynamic constants

Evaluation of the expressions obtained above requires knowledge of the various solubility constants. Furthermore, we intend to examine the temperature dependence of these relations. Data from Damidot and Glasser [6,7] are reported in Table 1.

The logarithm of the equilibrium constant varies linearly with the inverse of the absolute temperature as shown in Fig. 2. Additional data from Perkins and Palmer [18], who studied ettringite solubility in detail between 5 °C and 75 °C, are plotted in the same graph. Their results are relatively close to those obtained by Damidot and Glasser. Because we are interested in using simultaneously equilibrium constants of ettringite and another phase, we have chosen to use the data by Damidot and Glasser, which present the advantage of coming from a unique source.

3. Role of ettringite amount

Eqs. (5–7) and Fig. 1 show that hydrostatic tensile stress depends not only on the crystallization pressure but also on the amount of ettringite exerting that pressure at the pore scale. To

Table 1
Equilibrium constants reported by Damidot and Glasser [6,7]

	25 °C	50 °C	85 °C
Ettringite	$2.80\ 10^{-45}$	$2.24\ 10^{-43}$	$6.61\ 10^{-41}$
Monosulfate	$3.71\ 10^{-30}$	$1.48\ 10^{-29}$	$8.13\ 10^{-29}$
Hydrogarnet	$2.91\ 10^{-23}$	$1.26\ 10^{-22}$	$6.309\ 10^{-22}$
Gypsum	$3.72\ 10^{-5}$	$3.43\ 10^{-5}$	$2.35\ 10^{-5}$
Portlandite	$8.90\ 10^{-6}$	$4.57\ 10^{-6}$	$1.50\ 10^{-6}$

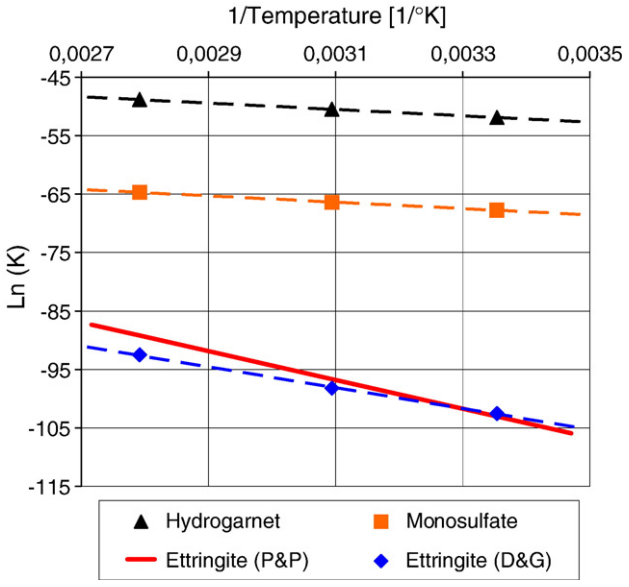

Fig. 2. Plot of ln(K) versus 1/T for monosulfate, hydrogarnet and ettringite. The discontinuous lines represent the linear fit to the data from Damidot and Glasser. The continuous line corresponds to ettringite, using the enthalpy and entropy of dissolution reported by Perkins and Palmer [18].

illustrate this semi-quantitatively, we examine heat treated mortar bars studied by Famy [19].

3.1. Experimental observations

Famy studied seven cements whose compositions are given in Table 2. Expansion measurements were done on 16×16×160 mm mortar bars. They were prepared with water (distilled)/cement=0.5 and sand (siliceous)/cement=3. After casting, the samples were tightly covered, placed sealed in plastic bags under water and pre-cured at 20 °C for 4 h. They were then cured at 90 °C for 12 h, with heating rates of 30–35 °C/h. After this, samples were left to cool naturally to 20 °C over about 5 h. They were then demolded and placed under water. Length change measurements were done periodically and their long term values are also given in Table 1. It should be noted that the samples that expand do so in large excess of the elastic limit of cementitious materials. Thus, the values of expansion are used directly as an indicator of damage and no quantification is (or should be) done to relate this to crystallization pressure of a material having a fixed constant strength.

Subsequently to this work, the expansive cement D was used to prepare mortar bars for determination of flexural strength. The samples were 160×40×40 mm bars and had the same heat treatment. Measurements were done shortly after cooling to room temperature and gave an average of 6.9 MPa on the 9 samples measured [V. Poupardin, personal communication, 2002].

Using Eq. (10) we find a conversion factor of about 1.95 between flexural and tensile strength. Thus it is estimated that the tensile strength of these mortar bars is about 3.5 MPa.

3.2. Theoretical considerations

To estimate the susceptibility of these mortar bars to DEF, we need to estimate their tensile strength at very low loading rates, as well as the hydrostatic tensile stress. The latter depends both on supersaturation and on the amount of ettringite exerting stress at the pore scale.

In this section, we first estimate the amount of ettringite exerting pressure and then the tensile strength at low loading rates. We then calculate the crystallization pressure expected in DEF. With these pressures and the tensile strength, we determine the amount of ettringite that would be needed for damage to occur. By comparing these values to those previously estimated, we find a rather good agreement between samples that either show or do not show expansion.

3.2.1. Volume fraction of crystals exerting pressure

The volume fraction of ettringite exerting pressure should be smaller than the total volume of ettringite. After heat curing, this amount can be estimated from the sulfate content of each cement. This means that we neglect the amount of monosulfate in the ultimate equilibrium phase assemblage. Based on the sulfate contents reported in Table 2, the water cement ratio and sand content used, the maximum amount of ettringite is estimated to be 3% to 6% by volume in these mortars. Together with Eqs. (5–7), this means that the crystallization pressure must be between 17 and 25 times larger than the long term tensile strength for damage, if crystals are forming in spherical pores with small entries. If they form in cylindrical pores, the crystallization pressure must be between 25 and 39 times larger than the long term tensile strength.

3.2.2. Long term tensile strength

For the samples that expand, dilatation begins after about 50–100 days. However, there are indications that ettringite forms rather rapidly. For this reason, we consider that the mortars are loaded for the whole period of time until damage develops. This means that we should use Eq. (11) with a loading duration to estimate the pertinent material strength. Doing this, we find that damage could occur if the hydrostatic tensile stresses reach only about 47% of the tensile strength obtained under normal laboratory loading rates.

Table 2
Composition of cements studied by Famy [19]

Cement	C3S	C2S	C3A	C4AF	Blaine	SO_3	Expansion	Ettringite in mortar
	%	%	%	%	%	%	%	%
D	55.2	21.2	10.8	6.7	337	3.9	1.0	5.5
D1	60.1	11.9	10.9	6.7	345	4.1	1.0	5.8
B	61.2	15.4	5.5	9.5	368	2.9	0.5	4.1
F	59.9	13	9.7	6.6	415	3.6	0.5	5.1
A	72.9	10.8	4.7	6.6	296	2.1	0.0	3.0
E	62.7	9.5	5.8	11.9	386	2.9	0.0	4.1
C	62.5	15.3	6.6	9.5	384	2.7	0.0	3.8
D+FA							0.0	4.5

Main phase composition, Blaine as well as SO_3 content and long term expansion are given. The SO_3 content is given, because it is used for estimation of the maximum possible amount of ettringite that can form in these cements. The sample D+FA corresponds to a blend of cement D with a fly-ash in proportions 4:1.

Table 3
Pore solution compositions from study by Famy [19] and resulting activities of species relevant for supersaturation of ettringite (assuming monosulfate equilibrium)

Cement	Pore solution composition [mmol/kgH_2O]				Activity at 20 °C			Q/K gypsum at 20 °C
	Ca	K	Na	SO_4	Ca	SO_4	H_2O	
A	20	25	10	20	4.76E-03	5.53E-03	0.998	0.76
B	20	240	50	40	2.07E-03	6.73E-03	0.99	0.39
D	30	440	60	150	2.55E-03	1.91E-02	0.985	1.36

These solutions were measured after heat treatment at 90 °C.
Hydroxyl concentrations were not reported by Famy. In the activity calculations, they were adjusted to satisfy electro neutrality.

This value should be used with care since the authors of that equation also indicate that the 90% confidence interval for the time to reach fracture is given as $\log_{10}(t_f)+/-1.70$. For the load decrease of 48% this would correspond to a time interval between 1 day and 7 years! However, for our concerns, it is good enough to observe that this corresponds to a range of strength decrease between 60% and 37%.

More importantly, we need to emphasize that the data leading to Eq. (11) were for separate samples altogether. Nevertheless, in the absence of more adequate data and for simplicity we use the above estimated strength decrease of ~50%, recognizing that there is an important uncertainty on this value. The tensile strength we use to analyze our results is therefore 1.75 MPa.

3.2.3. Crystallization pressure

Above, we proposed two limiting cases to evaluate the ettringite. These involve assuming that either gypsum or hydrogarnet is at equilibrium in addition to monosulfate. Apart from this, we could use pore solution analysis of these mortars given by Famy [19, page 132].Table 3 reports the approximate pore solution compositions of those three samples. Activities of calcium, sulfate and water were calculated using an extended Debye–Hückel approach [PHREEQ]. In these calculations, electrical neutrality is obtained by adjusting the pH. The supersaturation with respect to gypsum is calculated and found on average to be quite close to unity.

The pore water compositions in Table 3 are close to gypsum saturation as indicated in the last column of that table. This would reinforce the choice of assuming gypsum saturation. Nevertheless, at the location where crystals are growing, the concentration may be lower than the average obtained by pore solution analysis owing to the consumption of ions by crystal growth. This means that using pore solution analysis is not necessarily a better choice than assuming local equilibrium of well chosen phases. For this reason and for the sake of simplicity, we proceed with the equilibrium approach.

Assuming either gypsum or hydrogarnet saturation, we calculate crystallization pressure at 20 °C. For this we use solubility data from Table 1 and assume Van't Hoff law to be valid. With these values we calculate the expected crystallization pressures from Eq. (1) and values of 50 and 12 MPa respectively were obtained.

3.3. Linking theory and experimental observation

In this section we examine whether crystallization stresses estimated from theory can account for whether mortars expand or not. For this, we first calculate the volume fraction of ettringite needed for the hydrostatic tensile stress to exceed the tensile strength of these mortars at a low loading rate. We then compare this amount with values reported in Table 2 on the basis of the cement sulfate content.

If hydrogarnet equilibrium is assumed, we find that regardless of the pore shape, the amount of ettringite needed (13%–18%) largely exceeds the maximum value in Table 2 (6%). On the other hand, for gypsum equilibrium, we find values consistent with Table 2 between 3.4 and 4.9%, depending on the pore shape. This is in general agreement with Table 2 and Fig. 3. Indeed, that figure suggests the existence of a critical range of ettringite content around 4–5% for these mortars.

Another very interesting observation in Famy's work is that no expansion was obtained when a 4:1 blend of the expansive cement and fly-ash was used. Assuming no sulfates are provided by the fly-ash, the maximum ettringite content in the mortar shifts from 5.5% to 4.5%. This is represented in Fig. 3 by the arrow linking the filled to the open diamond. It is generally consistent with the previously estimated critical ettringite content range.

4. Role of storage temperature

4.1. Experimental results

Subsequently to Famy's thesis, the expansive cement D was used to study the role of storage temperature in similar mortar bars. The limited data presented here about these tests were provided to us by Lafarge Central Research (LCR) and were obtained with the procedure described above. In this case however,

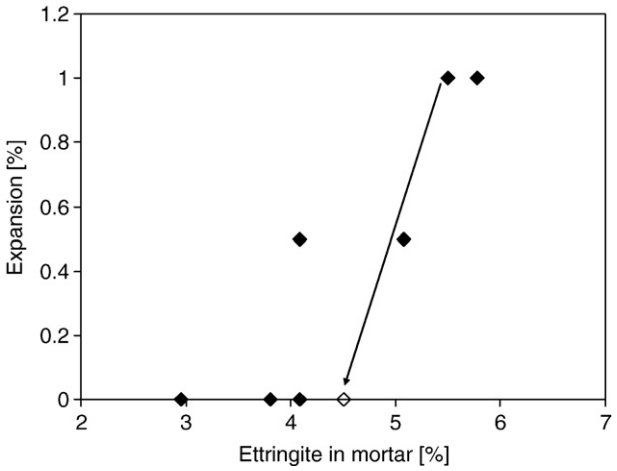

Fig. 3. Plot of linear expansion obtained by Famy [19] versus maximum amount of ettringite obtainable in the cement paste. The open symbol represents a blend in which an expansive cement is used in proportions of 4:1 with fly-ash. The arrow indicates the change undergone from the blending with fly-ash.

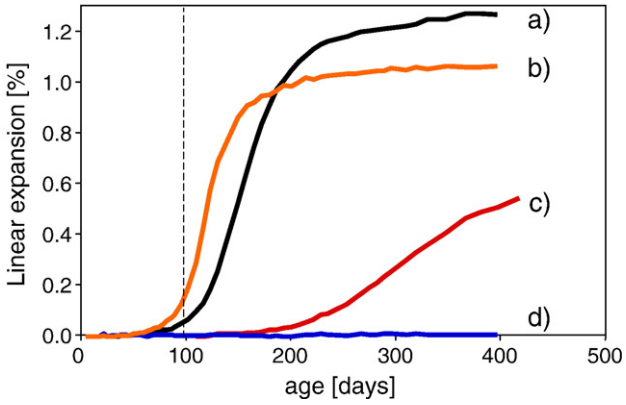

Fig. 4. Linear expansion of heat treated mortars having different heat treatments. Storage conditions were: a) 20 °C, b) 20 °C 98 days and then 38 °C, c) 38 °C 98 days then 20 °C, d) 38 °C. The discontinuous vertical line indicates the moment at which the storage temperatures of samples (b) and (c) were changed.

after cooling, the samples were placed in water either at 20 °C or 38 °C. After 98 days, the storage temperature of sample (c) was switched from 20 °C to 38 °C, whereas for sample (b), the opposite was done. Samples (a) and (d) remained respectively at 20 °C and 38 °C.

Results plotted in Fig. 4 show a role of storage temperature. Sample (a) was continuously at 20 °C and expanded. Sample (d) was at 38 °C and did not expand. Sample (c), which was switched from 38 °C to 20 °C after 98 days, started to expand after this change. Sample (b), which was switched from 38 °C to 20 °C, does not stop expanding after the change. However, in this case it had already substantially expanded before 98 days (Fig. 4). This means that it was probably damaged and much weaker by the time its storage temperature was changed.

Interestingly, the LCR researchers indicated that regardless of the storage temperature, similar amounts of ettringite were observed to form (no substantial difference in XRD or SEM). However, we do not know about possible differences in the location at which it formed. To understand this experiment, we present a stress evaluation as a function of storage temperature.

4.2. Theoretical considerations

In the absence of data on the role of storage temperature on strength, we use the same estimate for the long term strength at both temperatures. The long term strength (at loading rates on the order of the test duration) is plotted in Fig. 5 as the continuous horizontal line. Various cases are then considered for the expected hydrostatic tensile stress. These are obtained for two volume fractions of ettringite in mortar (3.7 and 5.6%, corresponding to 10 and 15% in the paste). In addition, both spherical and cylindrical pores are considered for each case (lower and upper curves, respectively). When the stress lines are above the strength lines, damage can be expected to occur.

Here only the case of gypsum equilibrium is considered, since the hydrogarnet equilibrium case leads to stresses below the sample strength, in agreement with the previous example. As before the equilibrium constants needed are calculated using solubility data from Table 1 and assuming the Van't Hoff law to be valid.

4.3. Linking theory and experimental observation

From Fig. 5 samples with 5.6% ettringite would be expected to cause damage over the whole temperature range, if crystals form in pores with small entries. If they form in cylindrical pores, a transition temperature between damage and no damage would be expected between 30 and 40 °C.

For samples with 3.7% ettringite, a similar transition temperature is found for spherical pores with small entries. With that lower amount of ettringite the stress would not be damaging if crystals were in cylindrical pores.

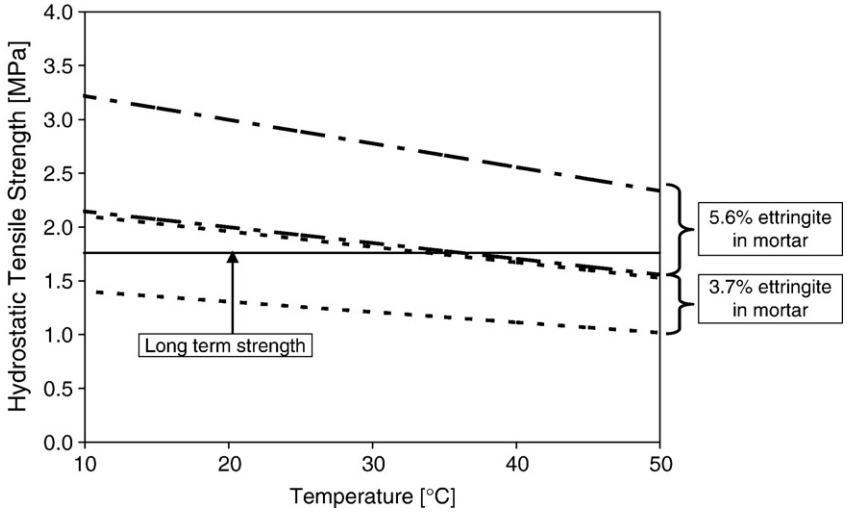

Fig. 5. Variation of estimated hydrostatic tensile stress that can be obtained in DEF. Temperature dependent values are reported for volume fractions of ettringite of 5.6% (discontinuous line) and 3.7% (dotted line) in the mortar, corresponding to 15% and 10% in the paste. In each pair of lines, the upper one represents the case of crystals confined in spherical pores with small entries and the lower line the case of crystals in cylindrical pores. The continuous horizontal line represents the long term strength of these mortars. If it is below the expected hydrostatic tensile stress then damage would be expected to happen.

The samples in Fig. 4 correspond to cement D and form a maximum of about 5.6% ettringite. Since all that ettringite is probably not exerting stress, the situation must be intermediate between the two cases in Fig. 5. Thus, we are generally consistent with the experimental observation that these mortars expand at 20 °C but not at 38 °C. The agreement is improved if we can assume that crystallization takes place in cylindrical pores.

5. Role of pore size and shape

We can estimate the equilibrium curvature of the crystal/liquid interface corresponding to the calculated supersaturations, using the Freundlich equation [20]:

$$\gamma_{CL}\kappa_{CL} = \frac{R_g T}{v_{crystal}} \ln\left(\frac{Q}{K}\right) \tag{22}$$

where γ_{CL} and κ_{CL} are respectively the interfacial energy and curvature of the crystal–liquid interface.

For a spherical pore with cylindrical entries of radius r, κ_{CL} is $2/r$. Using a value of 0.1 N m for γ_{CL}, and the supersaturation calculated at 20 °C for the gypsum equilibrium situation, we find r=4.0 nm. To get the maximum crystallization pressure assumed in Fig. 5, the minimum pore interior radius would have to be about 5 to 10 times larger than r. Therefore, crystals as small as 20 nm in radius could be responsible for DEF damage. Such crystals would be virtually invisible to XRD and SEM. In the event that enough crystals in cylindrical pores are present, the damage would occur with crystals as small as about 2 nm in radius.

Since the damage occurs on such a small scale, the stress development and crack initiation should occur in a similar way in the pure paste or in a cementitious composite. However, the transport properties and crack propagation would be influenced by the presence of aggregate.

6. Role of humidity

The stress created by precipitation of ettringite is given in Eq. (1) and shows that it is proportional to the logarithm of supersaturation. The estimations of supersaturation from Eqs. (16) and (19) depend primarily on the equilibrium constants of monosulfate, ettringite and hydrogarnet, which all vary differently with temperature.

There is a minor dependence on solution composition through water activity. This term will only become important in dry samples when it will reduce the crystallization stresses substantially. This is compatible with experimental observation. However, since the formation of ettringite most probably takes place through solution, water has to be present. This would explain why dry samples do not suffer DEF.

7. Role of pH

To examine qualitatively the role of hydroxyl concentration, the most convenient approach is to take the assumption of portlandite equilibrium in Eq. (21). This indicates that maintaining high hydroxyl concentration should limit the driving force for crystallization and therefore the extent of damage. This is compatible with the results from Famy et al. [21] in which they show that if a heat-cured mortar is placed in an alkaline solution, regardless of the nature of the counter-ion of the alkaline solution, then the expansion is reduced as the hydroxyl concentration is increased.

8. Role of solid solutions

Up to now we have considered that the aluminates are coming from monosulfate, a well defined sulfate version of the AFm structure. This is not the best picture of reality since, according to Glasser et al. [22], there can be a hydroxyl, chloride or carbonate substitution for sulfates in the structure of AFm. Though the range of substitution is not totally independent of molar fraction, it does occur throughout the composition range, so that it may be in a simplified way viewed as a solid solution.

It is not the objective here to bring additional arguments to the debate about the exact form of the partially substituted AFm structure, but rather to examine some interesting implications that result from solid solution thermodynamics and that might bring new light into why experimental data on DEF can sometimes be so contradictory from one study to another.

The thermodynamic treatment is outlined in Annex A. We only consider the situation of hydroxyl substitution in order to illustrate the effect that such substitutions can have. According to Matschei et al. [23,24], this is the only case of solution in AFm for the hydroxyl, sulfate and carbonate AFms. Furthermore the extent of hydroxyl substitution is limited to about 50%[2]. This is the situation of a binary solid solution we can note $A(B_b)_y(C_c)_{(1-y)}$ between minerals AB_b and AC_c, where y is the molar fraction of AB_b. Defining the sulfate AFm as the AB_b pole and hydroxyl AFm as the AC_c pole, and using Eq. (42), we get for the simple case of an ideal solid solution:

$$\frac{Q_{ettringite}}{K_{ettringite}} = \frac{K^3_{monosulfate}\, K^2_{portlandite}}{K_{ettringite} K^2_{AFm(OH^-)}} \frac{y^5}{(1-y)^2} a^{20}_{H_2O} \tag{23}$$

In this case, the variation of supersaturation is monotonic between both solid solution poles. Thus, an increasing amount of hydroxyls in the system (decreasing y) should decrease crystallization pressure. The role of solid solutions should therefore most likely not be overlooked. Further consideration of this appears to be an important challenge for durability studies.

9. Conclusions

We have outlined a simple approach to estimating driving forces for crystallization pressures. For mortars studied by Famy [19] we calculated that mortars containing less than about 3.5% confined and supersaturated ettringite by volume would

[2] These results by Matschei and Glasser contrast with previous reports in the literature about the existence of extensive AFm solid solutions. It should be emphasized that the studies in question do not include chlorides but only hydroxyls, carbonates and sulfates, which is the most pertinent subsystem for this paper.

not be expected to get damaged. If that amount rises to about 5.5%, then damage is definitely expected. In between there is a gray zone where several factors may matter and make prediction difficult. These are:

1) Storage temperature. In this case, we can account for the fact that an expansive mortar at 20 °C may be non-expansive at 38 °C, because of reduced supersaturation (Fig. 5).
2) Equilibrium of portlandite should decrease crystallization pressures, which is in qualitative agreement with observations that show that heat-cured samples are not damaged from DEF when they are stored in highly alkaline solutions. This effect should be increased by the possible partial solid solution between hydroxyl AFm and monosulfate.
3) The long term tensile strength. This factor is very important but few data exist for the time periods of interest.
4) The role of blends. At equal strength, a blend that does not contribute sulfates for ettringite formation may be considered as an ettringite diluter, which in several circumstances may be sufficient to avoid damage. It may also be possible that the time to reach critical stresses will increase because a higher proportion of the ettringite available will have to form under supersaturated conditions and kinetics of stress release by growth of unloaded crystals may become more important.
5) Amount of confined and supersaturated ettringite. If enough ettringite is formed, filled pores with entries smaller than 4 nm and internal radii larger than about 20 nm could lead to damaging stresses. Such crystals would be virtually invisible to XRD, which can explain why expansion is reported to be observed before ettringite is detectable by that method.

This study brought out two important aspects that have not yet received much attention:

1) In view of the strength decrease with time, the delay before expansion occurs in DEF is linked not only to leaching of alkalis and crystal growth, but also to the time needed for the material to fail at crystallization pressures that may have been reached and maintained long before.
2) Not only the confinement of ettringite and its supersaturation are necessary for crystallization pressure to be damaging in DEF. The sample strength must also be considered, as well as the volume fraction of ettringite that will be able to exert pressure because of confined growth. In this paper, we have used worst case approximations whereby the calcium sulphate content of cement is used to estimate that value. Clearly the situation is more complex and forgiving. However, it is worth pointing out that within the framework of this approximation it is easy to show that, the better performance of blends could simply be understood as “ettringite dilution effect”.

It is our impression that similar issues may be pertinent in other durability studies involving crystallization pressure. It is our hope that this paper will, beyond the scope of DEF, raise critical thought on this eventuality.

Acknowledgements

Support for Robert Flatt at the time this work was initiated was provided by Lafarge LCR. The authors are further grateful to Lafarge LCR for useful discussions and feedback on this work, particularly V. Poupardin, D. Sorentino, K. Scrivener (now at EPFL) and more recently G. Chanvillard.

Annex A

We examine the thermodynamics for the equilibrium between a liquid phase and a solid solution. For example, a solid solution between two components AB_b and AC_c would be written $A(B_b)_y(C_c)_{(1-y)}$. One mole of this solution would contain y moles of AB_b and $(1-y)$ moles of AC_c. We write the chemical potential $\mu_{j,S}$ of any pole j of the solid solution as:

$$\mu_{j,S} = \mu^0_{j,S} + R_g T \ln\left[a_{j,S}\right] \tag{24}$$

where $a_{j,S}$ and $\mu^0_{j,S}$ are respectively the activity and standard chemical potential of the poles in the solid solution.

At equilibrium, the free energy of the whole system must be minimized. At constant temperature and pressure this leads to:

$$\begin{aligned} dG = &\sum_{j=1}^{N_S}\left(\mu^0_{j,S} + R_g T \ln\left[a_{j,S}\right]\right) dn_{j,S} \\ &+ \sum_{i=1}^{N_L}\left(\mu^0_{i,L} + R_g T \ln\left[a_{i,L}\right]\right) dn_{i,L=0} \end{aligned} \tag{25}$$

where subscript i corresponds to the species in the aqueous phase, N_S is the total number of poles of the solid solution and N_L is the number of species in the liquid phase.

This can also be written in terms the number of moles of solid solution, n_S, and the molar fraction of component j in the solid solution $y_{,Sj}$.

$$\begin{aligned} &\sum_{j=1}^{N_S}\left(\mu^0_{j,S} + R_g T \ln\left[a_{j,S}\right]\right)\left(y_{j,S} dn_S + n_S dy_{j,S}\right) \\ &\quad = -\sum_{i=1}^{N_L}\left(\mu^0_{i,L} + R_g T \ln\left[a_{i,L}\right]\right) dn_{i,L} \end{aligned} \tag{26}$$

where n_S is the total number of moles of each pole of the solid solution. Let us write a mass balance of the species i in the system:

$$n_{i,T} = n_{i,L} + n_S \sum_{j=1}^{N_S} y_{j,S}\alpha_{i,j} \tag{27}$$

where $n_{i,T}$ and n_i are respectively the number of moles of species i in the whole system and in the liquid phase, and $\alpha_{i,j}$ is the stoichiometric coefficient of species i in the pole j of the solid solution.

The total number of species of i, $n_{i,\mathrm{T}}$, is constant, so we can write that:

$$\mathrm{d}n_{i,\mathrm{L}} = -\left(\sum_{j=1}^{N_\mathrm{S}} \alpha_{i,j} y_{j,\mathrm{S}}\right)\mathrm{d}n_\mathrm{S} - n_\mathrm{S}\sum_{j=1}^{N_\mathrm{S}} \alpha_{i,j}\mathrm{d}y_{j,\mathrm{S}} \tag{28}$$

Substitution into Eq. (26) gives,

$$\begin{aligned}\sum_{j=1}^{N_\mathrm{S}} y_j\left(\mu^0_{j,\mathrm{S}} + R_\mathrm{g}T\ln\left[a_{j,\mathrm{S}}\right]\right)\mathrm{d}n_\mathrm{S} + n_\mathrm{S}\left(\mu^0_{j,\mathrm{S}} + R_\mathrm{g}T\ln\left[a_{j,\mathrm{S}}\right]\right)\mathrm{d}y_{j,\mathrm{S}} \\ = \sum_{i=1}^{N_\mathrm{L}}\left(\mu^0_{i,\mathrm{L}} + R_\mathrm{g}T\ln\left[a_{i,\mathrm{L}}\right]\right)\left(\left(\sum_{j=1}^{N_\mathrm{S}}\alpha_{i,j}y_{j,\mathrm{S}}\right)\mathrm{d}n_\mathrm{S} \right. \\ \left. + n_\mathrm{S}\sum\nolimits_{j=1}^{N_\mathrm{S}}\alpha_{i,j}\mathrm{d}y_{j,\mathrm{S}}\right)\end{aligned} \tag{29}$$

or

$$\begin{aligned}\sum_{j=}^{N_\mathrm{S}} y_{j,\mathrm{S}}\left(\mu^0_{j,\mathrm{S}} + R_\mathrm{g}T\ln\left[a_{j,\mathrm{S}}\right] - \alpha_{i,j}\sum_{i=1}^{N_\mathrm{L}}\left(\mu^0_{i,\mathrm{L}} + R_\mathrm{g}T\ln\left[a_{i,\mathrm{L}}\right]\right)\right)\mathrm{d}n_\mathrm{S} \\ + n_\mathrm{S}\left(\sum_{i=1}^{N_\mathrm{S}}\left(\mu^0_{j,\mathrm{S}} + R_\mathrm{g}T\ln\left[a_{j,\mathrm{S}}\right] - \sum_{i=1}^{N_\mathrm{L}}\alpha_{i,j}\left(\mu^0_{i,\mathrm{L}} + R_\mathrm{g}T\ln\left[a_{i,\mathrm{L}}\right]\right)\right)\mathrm{d}y_{j,\mathrm{S}}\right) = 0\end{aligned} \tag{30}$$

The standard free energy for the dissolution of each pole of the solid solution is given by the standard chemical potential of its components and is linked to the equilibrium constant by:

$$\Delta G^0_j = \sum_{i=1}^{N_\mathrm{L}}\alpha_{i,j}\mu^0_{i,\mathrm{L}} - \mu^0_{j,\mathrm{S}} = -R_\mathrm{g}T\ln\left(K_j\right) \tag{31}$$

The solubility product with respect to pure j is:

$$Q_j = \prod_{i=1}^{N_\mathrm{L}} a_{i,\mathrm{L}}^{\alpha_{i,j}} \tag{32}$$

Eqs. (31) and (32) combine to:

$$\mu^0_{j,\mathrm{S}} - \sum_{i=1}^{N_\mathrm{L}}\alpha_{i,j}\left(\mu^0_{i,\mathrm{L}} + R_\mathrm{g}T\ln\left[a_{i,\mathrm{L}}\right]\right) = R_\mathrm{g}T\ln\left(\frac{K_j}{Q_j}\right) \tag{33}$$

Substitution into Eq. (30) leads to:

$$\sum_{j=1}^{N_\mathrm{S}} y_{j,\mathrm{S}}\ln\left[\frac{Q_j}{K_j a_{j,\mathrm{S}}}\right]\mathrm{d}n_\mathrm{S} + n_\mathrm{S}\left(\sum_{j=1}^{N_\mathrm{S}}\ln\left[\frac{Q_j}{K_j a_{j,\mathrm{S}}}\right]\mathrm{d}y_{j,\mathrm{S}}\right) = 0 \tag{34}$$

For a binary solid solution $A(B_\mathrm{b})_y(C_\mathrm{c})_{(1-y)}$ of minerals AB_b and AC_c that dissociate in the aqueous phase to A, B and C, we get:

$$\begin{aligned}\ln\left[\left(\frac{Q_{AB}}{K_{AB}a_{AB}}\right)^y\left(\frac{Q_{AC_\mathrm{c}}}{K_{AC_\mathrm{c}}a_{AC_\mathrm{c}}}\right)^{1-y}\right]\mathrm{d}n_\mathrm{S} \\ + n_\mathrm{S}\ln\left[\left(\frac{Q_{AB}}{K_{AB}a_{AB}}\right)\left(\frac{Q_{AC_\mathrm{c}}}{K_{AC_\mathrm{c}}a_{AC_\mathrm{c}}}\right)^{-1}\right]\mathrm{d}y = 0\end{aligned} \tag{35}$$

Free energy must be minimized with respect to both molar fraction and number of moles of solid solution so we get

$$\left(\frac{Q_{AB}}{K_{AB}a_{AB}}\right)\left(\frac{Q_{AC_\mathrm{c}}}{K_{AC_\mathrm{c}}a_{AC_\mathrm{c}}}\right)^{\frac{1-y}{y}} = 1 \tag{36}$$

and

$$\left(\frac{Q_{AB}}{K_{AB}a_{AB}}\right)\left(\frac{Q_{AC_\mathrm{c}}}{K_{AC_\mathrm{c}}a_{AC_\mathrm{c}}}\right)^{-1} = 1 \tag{37}$$

Dividing one by the other gives:

$$\left(\frac{Q_{AC_\mathrm{c}}}{K_{AC_\mathrm{c}}a_{AC_\mathrm{c}}}\right)^{\frac{1}{y}} = 1 \tag{38}$$

or

$$\frac{Q_{AC_\mathrm{c}}}{K_{AC_\mathrm{c}}a_{AC_\mathrm{c}}} = 1 \tag{39}$$

also implying that:

$$\frac{Q_{AB}}{K_{AB}a_{AB}} = 1 \tag{40}$$

Let us now consider the case in which monosulfate is forming a binary solid solution. We would have to replace the equilibrium constant of monosulfate by its ion activity product in the expressions developed earlier. In the case of simultaneous hydrogarnet equilibrium, Eqs. (12), (17) and (40) lead to:

$$\frac{Q_\mathrm{ettringite}}{K_\mathrm{ettringite}} = \frac{K^3_\mathrm{monosulfate}}{K_\mathrm{ettringite}\,K^2_\mathrm{hydrogarnet}}a^3_{\mathrm{AFm}\left(\mathrm{SO}_4^{2-}\right)}a^8_{\mathrm{H_2O}} \tag{41}$$

where $a^3_{\mathrm{AFm}\left(\mathrm{SO}_4^{2-}\right)}$ is the activity of the sulfate pole of the AFm solid solution. Thus if the solid solution is ideal and there is a simultaneous equilibrium of hydrogarnet then substitution should decrease crystallization pressure.

In the case of portlandite equilibrium, we would get:

$$\frac{Q_\mathrm{ettringite}}{K_\mathrm{ettringite}} = \frac{K_\mathrm{monosulfate}\,K^2_\mathrm{portlandite}}{K_\mathrm{ettringite}}a^3_{\mathrm{AFm}\left(\mathrm{SO}_4^{2-}\right)}\frac{a^2_{\mathrm{SO}_4^{2-}}}{a^4_{\mathrm{OH}^-}}a^{20}_{\mathrm{H_2O}} \tag{42}$$

In this case we must take into account that substitution of sulfates by another anion decreases $a^3_{\mathrm{AFm}\left(\mathrm{SO}_4^{2-}\right)}$, but increases $a^2_{\mathrm{SO}_4^{2-}}$. Because our objective here is only to demonstrate the general effect of possible ion substitution, we only consider the case where those anions are hydroxides. We must consider the variation of concentrations of sulfates and hydroxyls. In fact if we divide Eq. (40) by (39) we can write:

$$\frac{Q_{\mathrm{AFm}\left(\mathrm{SO}_4^{2-}\right)}}{Q_{\mathrm{AFm(OH^-)}}} = \frac{K_{\mathrm{AFm}\left(\mathrm{SO}_4^{2-}\right)}a_{\mathrm{AFm}\left(\mathrm{SO}_4^{2-}\right)}}{K_{\mathrm{AFm(OH^-)}}a_{\mathrm{AFm(OH^-)}}} = \frac{a_{\mathrm{SO}_4^{2-}}}{a^2_{\mathrm{OH}^{2-}}} \tag{43}$$

Assuming an ideal solid solution, substitution into Eq. (42) gives:

$$\frac{Q_\mathrm{ettringite}}{K_\mathrm{ettringite}} = \frac{K^3_\mathrm{monosulfate}\,K^2_\mathrm{portlandite}}{K_\mathrm{ettringite}K^2_{\mathrm{AFm(OH^-)}}}\frac{y^5}{(1-y)^2}a^{20}_{\mathrm{H_2O}} \tag{44}$$

Annex B

In this article we have proposed various ways to estimate the supersaturation of ettringite during DEF. This is done by assuming the equilibrium of various phases. We have found that crystals as small as 20 nm in radius could be responsible for pressure that would damage many cementitious materials.

If the dissolving crystals that provide ions for the growth of the destructive crystals are located in pores of similar sizes then their solubility will be higher and so would be the crystallization pressure of ettringite. A similar situation would occur if the ettringite were pressing on those crystals, both then being confined in the same pores.

The simplest approach for quantifying this is to assume that the reacting crystals are at the same pressure as the growing crystals. This can occur as mentioned above if ettringite is pressing on the reacting crystals or if the crystals are of similar size and have similar crystal–liquid interfacial energies.

In a first stage, we will only consider monosulfate as not being at ambient pressure. We rewrite Eqs. (1) and (16) as:

$$\sigma_C = \sigma_{C,\text{ettringite}} = \frac{R_g T}{v_{\text{ettringite}}} \ln\left(\frac{Q_{\text{monosulfate}} K_{\text{gypsum}}^2}{K_{\text{ettringite}}} a_{H_2O}^{16}\right) \quad (45)$$

where the activity product of monosulfate $Q_{\text{monosulfate}}$ is now obtained by stating that it is at the same pressure as ettringite:

$$\sigma_{C,\text{monosulfate}} = \sigma_C = \frac{R_g T}{v_{\text{monosulfate}}} \ln\left(\frac{Q_{\text{monosulfate}}}{K_{\text{monosulfate}}}\right) \quad (46)$$

Substitution of Eqs. (46) into (45) leads to:

$$\sigma_C = \frac{R_g T}{v_{\text{ettringite}} - v_{\text{monosulfate}}} \ln\left(\frac{K_{\text{monosulfate}} K_{\text{gypsum}}^2}{K_{\text{ettringite}}} a_{H_2O}^{16}\right) \quad (47)$$

The molar volume of ettringite is 735 cm^3/mol, while that of monosulfate is 313 cm^3/mol. It results that values from Eq. (47) are about 70% larger than when supersaturation is estimated from Eq. (16). Conversely, pores about 70% smaller than those discussed in the text could be responsible for damaging stresses.

We may of course take a similar approach for gypsum. This step appears, however, more questionable in that during the heat curing calcium and sulfate ions are expected to be much more homogeneously distributed throughout the porous network. As a result we would not expect too big departures from the activity product of calcium and gypsum estimated from pore solution analysis and which was found to be close to gypsum at ambient pressure. Nevertheless, we give the result, because it corresponds to the upper bound of ettringite crystallization pressure:

$$\sigma_C = \frac{R_g T}{v_{\text{ettringite}} - v_{\text{monosulfate}} - 2v_{\text{gypsum}}} \ln\left(\frac{K_{\text{monosulfate}} K_{\text{gypsum}}^2}{K_{\text{ettringite}}} a_{H_2O}^{16}\right) \quad (48)$$

The volume of gypsum being 74 cm^3/mol, results that pressures estimated from Eq. (48) are about 2.5 times larger than estimated from Eq. (16). Whether this is or is not a realistic situation is to be further studied.

We can also comment on the fact that the difference in molar volumes in Eq. (48) corresponds more or less to the volume of the 16 water molecules appearing as exponent for water activity in that equation. This result is fully consistent with other minerals [25]. It once again confirms that a phase change of a mineral or mineral assemblage leading to the formation of higher hydrates by consumption of water does not lead to high crystallization pressures because of the number of water molecules consumed, but because of the difference in thermodynamic stability of the reactants and products [25].

References

[1] H.F.W. Taylor, C. Famy, K.L. Scrivener, Delayed ettringite formation, Cem. Concr. Res. 21 (2001) 683–693.
[2] G.W. Scherer, Factors affecting crystallization pressure, in: K. Scrivener, J. Skalny (Eds.), Internal Sulfate Attack and Delayed Ettringite Formation, Proc. Int. RILEM 186-ISA Workshop, PRO 35, RILEM publications, Paris, 2004, pp. 139–154.
[3] G.W. Scherer, Stress from crystallization of salt, Cement Concr. Res. 34 (2004) 1613–1624.
[4] G.W. Scherer, Crystallization in pores, Cem. Concr. Res. 29 (1999) 1347–1358.
[5] G.W. Scherer, Stress from crystallization of salt in pores, in: V. Fassina (Ed.), Proceedings of the 9th International Congress on Deterioration and Conservation of Stone, Venice, June 19–25, Elsevier, Amsterdam, 2000, pp. 187–194.
[6] D. Damidot, F.P. Glasser, Thermodynamic investigation of the CaO–Al_2O_3–$CaSO_4$–H_2O system at 50 °C and 85 °C, Cem. Concr. Res. 22 (76) (1992) 1179–1191.
[7] D. Damidot, F.P. Glasser, Thermodynamic investigation of the CaO–Al_2O_3–$CaSO_4$–H_2O system at 25 °C, Cem. Concr. Res. 23 (1) (1993) 221–238.
[8] C.W. Correns, Growth and dissolution of crystals under linear pressure, Disc. Faraday Soc. 5 (1949) 267–271.
[9] R.J. Flatt, M. Steiger and G.W. Scherer A commented translation of the paper by C.W. Correns and W. Steinborn on crystallization pressure, Env. Geol. (in press).
[10] M. Steiger, Crystal growth in porous materials—II: Influence of crystal size on the crystallization pressure, J. Cryst. Growth 282 (2005) 455–469.
[11] Olivier Coussy, Poromechanics of freezing materials, J. Mech. Phys. Solids 53 (2005) 1689–1718.
[12] Olivier Coussy, Deformation and stress from in-pore drying-induced crystallization of salt, J. Mech. Phys. Solids 54 (2006) 1517–1547.
[13] G.W. Scherer, Freezing gels, J. Non-Cryst. Solids 155 (1993) 1–25.
[14] S.P. Timoshenko, J.N. Goodier, Theory of elasticity, 3rd Ed., McGraw-Hill, NewYork, 1970.
[15] T.C. Lu, J. Yang, Z. Suo, A.G. Evans, R. Hecht, R. Mehrabian, Matrix cracking intermetallic composites caused by thermal expansion mismatch, Acta Metall. Mater. 39 (8) (1991) 1883–1890.
[16] H. Tada, P.C. Paris, G.R. Irwin, The Stress Analysis of Cracks Handbook, Del Research, St. Louis, MO, 1985.
[17] Rheinhardt H.W. and Conrelissen H.A.W. (1985) Zeitstandzugversuche an Beton, In: Baustoffe ,85: Karlands Wechse gewidmet. Wiesbaden: Bauverlag, pp. 162–167.
[18] Perkins, Palmer, Solubility of ettringite ($Ca_6[Al(OH)_6]_2(SO_4)_3 \cdot 26H_2O$) at 5–75 °C, Geochim. Cosmochim. Acta 63 (1999) 1969–1980.
[19] C. Famy, Expansion of heat-cured mortars, PhD thesis, Imperial College of Science, Technology and Medicine (University of London) (1999).
[20] J. Freundlich, Colloid & Capillary Chemistry, Methuen, London, 1926, pp. 154–157.
[21] C. Famy, K.L. Scrivener, A. Atkinson, A.R. Brough, Influence of the storage conditions on the dimensional changes of heat-cured mortars, Cem. Concr. Res. 31 (2001) 795–803.

[22] F.G. Glasser, A. Kindness, S.A. Stronach, Stability and solubility relationships in AFm phases, Part I. Chloride, sulfate and hydroxide, Cem. Concr. Res. 29 (1999) 861–866.
[23] Matschei T., Lothenbach B. Glasser F.P. (in press), The AFm-phase in Portland cement, Cem Concr Res.
[24] Matschei T., Lothenbach B. Glasser F.P. (in press), The role of calcium carbonate in cement hydration, Cem Concr Res.
[25] R.J. Flatt, G.W. Scherer, hydration and crystallization pressure of sodium sulfate: a critical review, Mater. Res. Soc. Symp. Proc. 712 (2002) 29–34.
[26] FIB: Structural Concrete, Textbook on behaviour, design and performance, Updated knowledge of the CEB/FIP Model Code 1990, FIB bulletin 1, July 1999.
[27] R.J. Flatt, Salt damage in porous materials: how high supersaturations are generated, J. Cryst. Growth 242 (2002) 435–454.